

Effect of Degradation on Mechanical Strengths of Alkali-Activated Fines in Stabilized Construction and Demolition Waste Aggregates

Original

Effect of Degradation on Mechanical Strengths of Alkali-Activated Fines in Stabilized Construction and Demolition Waste Aggregates / Tefa, L.; Bassani, M.; Coppola, B.; Palmero, P.. - In: JOURNAL OF MATERIALS IN CIVIL ENGINEERING. - ISSN 0899-1561. - ELETTRONICO. - 34:2(2022), pp. 04021454-1-04021454-13. [10.1061/(ASCE)MT.1943-5533.0004090]

Availability:

This version is available at: 11583/2944612 since: 2021-12-13T08:18:11Z

Publisher:

American Society of Civil Engineers (ASCE)

Published

DOI:10.1061/(ASCE)MT.1943-5533.0004090

Terms of use:

This article is made available under terms and conditions as specified in the corresponding bibliographic description in the repository

Publisher copyright

ASCE postprint/Author's Accepted Manuscript

This material may be downloaded for personal use only. Any other use requires prior permission of the American Society of Civil Engineers. This material may be found at [http://dx.doi.org/10.1061/\(ASCE\)MT.1943-5533.0004090](http://dx.doi.org/10.1061/(ASCE)MT.1943-5533.0004090).

(Article begins on next page)

Effect of degradation on mechanical strengths of alkali-activated fines in stabilized construction and demolition waste aggregates

Luca Tefa*, Marco Bassani, Bartolomeo Coppola, Paola Palmero

Luca Tefa (* = corresponding author)

Research Fellow

Politecnico di Torino, Department of Environment, Land and Infrastructure Engineering

24, corso Duca degli Abruzzi, Torino, Italy, 10129

Phone: +39 011 090 5623, email: luca.tefa@polito.it

Marco Bassani

Associate professor

Politecnico di Torino, Department of Environment, Land and Infrastructure Engineering

24, corso Duca degli Abruzzi, Torino, Italy, 10129

email: marco.bassani@polito.it

Bartolomeo Coppola

Research Fellow

Politecnico di Torino, Department of Applied Science and Technology

24, corso Duca degli Abruzzi, Torino, Italy, 10129

email: bartolomeo.coppola@polito.it

Paola Palmero

Full Professor

Politecnico di Torino, Department of Applied Science and Technology

24, corso Duca degli Abruzzi, Torino, Italy, 10129

email: paola.palmero@polito.it

ABSTRACT

In recent works, the authors have demonstrated that construction and demolition waste (CDW) aggregates for subbase road pavement applications can be stabilized vis-à-vis the alkali-activation of their fine fraction ($d < 0.125$ mm). Despite the promising results with this method, the durability of alkali-activated CDW fines (which act to stabilize the CDW aggregate mixtures) need to be investigated. With this objective, the effects on pavement materials due to the typical degrading actions of water, de-icing salts, and the freeze-thaw process were investigated. Samples of alkali-activated (AA) fines were subjected to water, de-icing salt and freeze-thaw treatments and assessed as per the variation in 28-day flexural and compressive strength values with respect to non-degraded materials. In addition to the fines normally present in CDW aggregate mixtures (i.e., the undivided fraction), samples with fines of the main CDW constituents (concrete, asphalt, bricks and tiles, aggregates and soil) were also prepared for comparison purposes. One set of specimens was cured at 20 °C to replicate field conditions, and another was treated at 80 °C to replicate optimal conditions for AA materials. Although 80 °C heat-treated specimens achieved higher strength values, those values fell sharply following the degrading action of water and de-icing salts. In contrast, the specimens cured at 20 °C retained their mechanical property values even after exposure to water and de-icing salt degradations.

KEYWORDS

construction and demolition waste recycled aggregates, alkali-activation, durability, freeze-thaw degradation, water immersion, de-icing salt attack

INTRODUCTION

Construction and demolition waste (CDW) accounts for one-third of the total volume of waste produced in Europe (Bilsen et al. 2018). It mainly derives from the renovation and demolition (frequently micro-demolition) of buildings and roads and contains a mix of crushed concrete particles (RC), reclaimed asphalt (RA) pavement grains, ceramic products such as crushed bricks and tiles (BT), natural aggregates and excavated soils (NA), and occasional negligible amounts of impurities (i.e., glass, wood, metals, and plastic). In accordance with the European objectives of Circular Economy (European Environment Agency 2020), many countries have recently increased their rate of CDW recycling, using the mineral part of this waste source as recycled aggregate in partial or total substitution of natural resources (Di Maria et al. 2018). Due to the large volume involved, the highest proportion of CDW aggregate is currently employed in road pavements as granular material in the formation of unbound layers (Cardoso et al. 2016). Several studies have shown that the mechanical and durability properties of subbase pavement layers made up of CDW aggregates can be enhanced with the addition of minor quantities of binders as stabilizers. Although Ordinary Portland Cement (OPC) and blended hydraulic cements are the most widely used for stabilization purposes (Agrela et al. 2012; Mohammadinia et al. 2014), alternatives such as cement kiln dust (Bassani et al. 2016), fly ash (FA) (Arulrajah et al. 2017; Camargo et al. 2013), and alkali-activated (AA) by-products (Arulrajah et al. 2016; Cristelo et al. 2018; Mohammadinia et al. 2016) are attracting increasing interest for environmental reasons (McLellan et al. 2011; van Deventer et al. 2010). Despite the fact that the alkali-activation process has traditionally involved the use of reactive precursors which are amorphous or poorly crystallized aluminosilicates, e.g. blast furnace slag (BFS), FA, and calcined clays (Duxson et al. 2007), some studies investigated the feasibility of producing AA binders starting from mineral wastes with a highly crystalline structure (Palmero et al. 2017; Coppola et al. 2020b) and also including fine particles of CDW fines (Bassani et al. 2019a; Panizza et al. 2018; Allahverdi and Kani 2013; Zaharaki et al. 2016). Previous studies on AA-CDW fines explored the potential for the alkali-activation of cementitious (RC) and ceramic (BT) particles only of CDW (Robayo-Salazar et al. 2017; Vásquez et al. 2016; Reig et al. 2013).

Problem statement

Fig. 1 shows a road pavement with the subbase layer made up of stabilized CDW aggregates. According to a previous study (Bassani et al. 2019b), the full mixture of coarse and fine CDW aggregate particles can be stabilized through the alkaline activation of the aluminosilicates present in the finer fraction ($d < 0.125$ mm) without the addition of external reactive precursors. According to Komnitsas et al. (2015) and Ruiz-Santaquiteria et al. (2013), the AA of coarser particles is less effective. The addition of the chemical activator (alkaline solution) to the full mixture (coarse and fine CDW grains together) triggers the AA process within the fines, thus forming a new stabilizing phase that helps coarser particles to bond together thereby stabilizing the whole mixture.

Adopting this approach, Bassani et al. (2019a) and Tefa et al. (2021) investigated the alkali-activation potential of the finest fraction ($d < 0.125$ mm) only of CDW aggregates (named UND1). They found satisfactory strength values when comparing the chemical and mechanical properties of the AA-UND1 material with those obtained from the AA of fines ($d < 0.125$ mm) of CDW aggregate constituent materials (RC, RA, BT, and NA). In the framework of using CDW aggregates for road applications, typical thermal curing conditions in field roadworks (5, 20, and 40 °C) were replicated. Taking into account that the dissolution and consequent reactivity of raw powders in the alkaline medium is improved with thermal curing at temperatures higher than 70°C (Komnitsas et al. 2015; Sun et al. 2013), the effects of 80 °C treatment during curing were also explored (Tefa et al. 2021).

In addition to traffic loads, the mechanical properties of stabilized subbase layers of road pavements are weakened by environmental degradation. In fact, durability (i.e., the ability of a material to retain its original properties over time notwithstanding the environmental and load conditions it is subject to while in service) is one of the main concerns as regards pavement materials, particularly for those including recycled products (Karlsson and Isacson 2006; Mirza 2006; Silva 2012; Huda and Shahria Alam 2015; Avirneni et al. 2016; Guo et al. 2018). If rainwater infiltrates the pavement surface and/or rises from groundwater (Lee et al. 2004; Sangsefidi et al. 2019), it can wash away the stabilizer agent or interact with it thereby modifying its properties (Avirneni et al. 2016). Furthermore, water infiltration brings with it substances accumulated on the pavement surface such as de-icing salts (Cunningham et al. 2008). For instance, when calcium

chloride (CaCl_2) is employed as a de-icing agent in winter road maintenance, it tends to react with the $\text{Ca}(\text{OH})_2$ in hydrated cement forming unstable and expansive calcium oxychloride (Farnam et al. 2015).

In addition, the combination of water and cyclical freezing and thawing actions is another significant degrading factor which compromises the durability of road materials as a result of the increased volume of water in the permeable voids (Bassani and Tefa 2018; Bozyurt et al. 2013; Khoury and Zaman 2007).

Although AA binders are emerging as a promising alternative to OPC and blended hydraulic cements (Li et al. 2010; Bernal and Provis 2014), there are a few discordant opinions concerning their durability due to the lack of experimental investigations (Komnitsas and Zaharaki 2007; Juenger et al. 2011; Pacheco-Torgal et al. 2012). Moreover, there are no systematic investigations into the durability of AA products derived from CDW fine precursors.

Study objectives

This experimental study is aimed at investigating the effects of environmental degradation on the alkali-activated finer particles ($d < 0.125$ mm) of undivided CDW aggregates (here coded as UND1). From the perspective of stabilizing full CDW aggregate mixtures for the subbase layer of semi-rigid pavements, this stabilizing phase (i.e., the AA-UND1) was subjected to degrading phenomena such as (i) immersion in water, (ii) exposure to CaCl_2 , and (iii) freeze/thaw (F/T) cycles (Fig. 2).

This experimental investigation focused exclusively on the stabilizing phase of AA-CDW aggregate mixtures (Fig. 2-a). In order to have greater control over the experimental outcomes, the effects of degrading actions were assessed on AA-CDW fines only, rather than on the full mixture (which also includes coarse grains). With this decision on the experimental design, any secondary effects of other mixture-related factors were excluded a priori.

In this study, the durability of the undivided fine fraction of CDW aggregate (UND1) mixtures was compared to that of CDW constituent fines (RC, RA, BT, NA). The aim is to understand the response of each alkali-activated constituent and determine its specific contribution to the durability of AA-UND1 material. A further sample produced by mixing milled particles finer than 0.125 mm of RC,

RA, BT, and NA in equal quantities (named UND2) was also included in the comparative analysis due to the unknown nature of UND1.

Durability tests were carried out on specimens made from particles smaller than 0.125 mm, activated with an alkaline solution of sodium silicate and sodium hydroxide, and cured for 28 days at 20 °C (this temperature is representative of average roadwork applications). To explore the effects of degradation on AA materials in their optimal curing condition, durability tests were also conducted on a set of specimens treated at 80 °C for 48 hours. The effects of degradation were evaluated in terms of the variation in flexural and compressive strength values with respect to non-degraded (reference) samples (Fig. 2-b). From a practical point of view, the outcomes of this experimental investigation reveal the ability of the stabilizing phase of AA-CDW aggregate mixtures to retain its mechanical properties after the occurrence of degrading phenomena.

MATERIALS AND METHODS

Materials

CDW aggregates in the 0-25 mm size fraction were collected at a stationary recycling plant located in the metropolitan area of Turin, which processes waste from the demolition and renovation of buildings and civil infrastructures through crushing, cleaning, and sieving operations.

The two size fractions of UND1 were first extracted by sieving the 0-25 mm CDW aggregate sample at 0.125 and 0.063 mm and then combined in proportions of equal mass to form the starting precursor powder. The maximum size of particles (i.e., 0.125 mm) was determined in accordance with literature (Komnitsas et al. 2015; Ruiz-Santaquiteria et al. 2013; Bassani et al. 2019a). It is worth noting that fine precursors with a high specific surface are more reactive in the AA processes (Assi et al. 2018; Temuujin et al. 2009).

To obtain samples of RC, RA, BT, NA powders, particles larger than 10 mm were visually separated and then pulverized in a rotatory drum (Tefa et al. 2021). Powders of separated CDW constituents were sieved to obtain the two size fractions ($d < 0.063$ mm, and $0.063 \leq d < 0.125$ mm), which were afterwards mixed in proportions of equal mass (50% each). The undivided sample UND2

was prepared with a combination of RC, RA, BT, and NA fines (25% of mass each), with each of the four fines composed of the two size fractions in a 50/50 ratio.

The separation of CDW constituents, and subsequent pulverization and sieving operations, were carried out at laboratory scale for experimental purposes. It is worth noting that in full scale applications these additional operations are not required since UND1 is the finest fraction normally included in CDW aggregate mixtures.

The alkaline solution (AS) was obtained by combining sodium silicate (Na_2SiO_3) and sodium hydroxide (NaOH). In the first stage, flakes of sodium hydroxide (purity > 98%) were diluted in an equivalent mass of distilled water. Then, liquid sodium silicate (Na_2SiO_3), with a $\text{SiO}_2/\text{Na}_2\text{O}$ mass ratio of 3.4 and pH of 11.6, was added to the NaOH solution in a 4:1 mass ratio. The AS was cooled down to room temperature before being used in the specimen preparation (Palmero et al. 2017).

Chemical-physical characterizations of CDW fines

The finest fractions of CDW powders ($d < 0.063$ mm) were subjected to X-ray fluorescence analysis (XRF) to evaluate their chemical composition. Results (Table 1) confirmed the presence of a relevant amount of SiO_2 and Al_2O_3 in all constituents in line with the findings of a previous investigation (Bassani et al. 2019a) and literature (Bianchini et al. 2005; Angulo et al. 2009; Saiz Martínez et al. 2016; Courard et al. 2020). RC contains the highest amount of CaO (23.5%) due to the presence of calcium-rich aggregates and residual cement particles in this fraction, in line with Puthussery et al. (2017) and Limbachiya et al. (2007). The UND1 and UND2 fines are almost identical in terms of chemical composition, with significant amounts of SiO_2 (around 40%) and Al_2O_3 (equal to 12.2% and 8.7% for UND1 and UND2 respectively). This finding suggests that UND1 is primarily composed of particles of the four main constituents (i.e. RC, RA, BT, and NA). However, it is worth mentioning that minor quantities of unidentified material are usually present in the undivided fraction UND1 (Bassani et al. 2019a).

The particle size distribution shown in Fig. 3 was determined by applying the laser granulometer method directly to recombined samples (i.e. samples composed in equal measure of the two size fractions $d < 0.063$ mm and $0.063 \leq d < 0.125$ mm).

Table 2 provides the particle density (ρ_p) and intergranular porosity of dry compacts (v) measured on samples produced with 50% in mass of the two size fractions ($d < 0.063$ and $0.063 \leq d < 0.125$ mm) calculated as per the EN 1097-7 (European Committee for Standardization 2008a) and EN 1097-4 (European Committee for Standardization 2008b) respectively. The highest values of ρ_p were exhibited by NA and BT particles, while the lowest ones were recorded for RC and RA due to residual particles of cement or bitumen, respectively, adhering to aggregates and characterized by low densities (Katz 2003; Loria et al. 2009). RA and NA had the lowest v values, suggesting that these particles bind together better than particles of other constituents; UND1 and UND2 particles exhibit intermediate values.

Specimen preparation and curing

Specimens for mechanical tests and degradation simulations were prepared by mixing raw powder and AS in a liquid-to-solid ratio of 0.4 in accordance with previous investigations (Komnitsas 2016; Bassani et al. 2019a; Tefa et al. 2021).

Prismatic specimens of 80×20×20 mm size were prepared by pouring the mixture into plastic split moulds. Specimens were formed in two layers; each layer was compacted with a small rod, and the surface was levelled with a spatula.

Specimens were cured for 28 days under different conditions depending on the specific constituents and the thermal treatment desired (20 or 80 °C). The temperature of 20 °C represents the average field thermal curing condition, while 80 °C is considered the optimal temperature to promote the AA of precursors derived from CDW materials (Komnitsas et al. 2015).

In a preliminary testing phase, the time required for the AA-RA, AA-BT, and AA-NA specimens to harden was longer than that for AA-RC, AA-UND1, and AA-UND2. Hence, to promote the hardening of RA, BT, and NA specimens, they were first left to cure at 20 °C with relative humidity (RH) < 50% for 7 days after casting and then cured at room temperature and RH > 90%. In contrast, UND1, UND2, and RC samples were cured continuously at room temperature (20 °C) and with RH > 90% for 28 days (Fig. 4-a). Thermally treated specimens were exposed to 80 °C for the first 48

hours after casting (Fig. 4-b). Fig. 4 evidences that all samples were stored at 20 °C and RH > 90% for at least 21 days before the start of the mechanical testing phase.

Degradation simulation

After 28 days of curing, specimens were subjected to degradation by (i) immersion in water, (ii) the corrosive action of de-icing salts, and (iii) freeze-thaw (F/T) cycles. In the case of immersion in water, samples were placed in a plastic container and immersed in distilled water (around 0.6 litres per container). The immersion in water lasted for 5 days, after which specimens were left to dry for 24 hours and then subjected to mechanical tests.

The same procedure was used for de-icing salt degradation. An aqueous solution prepared by mixing 4 g of anhydrous powder of CaCl₂ in 100 ml of distilled water (concentration of 4%) was used as per ASTM C672 (ASTM International 2012).

The degradation due to freezing was simulated by exposing hardened specimens to 12 F/T cycles of 48 hours between temperatures of $-(20\pm 1)^{\circ}\text{C}$ to $+(20\pm 1)^{\circ}\text{C}$. F/T degradation is usually administered to specimens completely immersed in water (Komnitsas et al. 2015; Komnitsas 2016; Topçu et al. 2014; Degirmenci 2017). However, this testing approach fails to recreate the conditions to which the material could be exposed in the subbase layer of road pavements. In such applications, the material is usually below an impervious layer containing the bituminous mixture and far from the groundwater (Bassani and Tefa 2018; Bilodeau et al. 2011; Tian et al. 2019). For these reasons, hardened specimens were directly placed into a thermal cabinet and exposed to F/T cycles without immersion in water.

A set of AA specimens (5 replicates) of each constituent was not subjected to the degrading procedure but underwent mechanical tests directly after 28 days of curing to define the reference properties for non-degraded material.

Mechanical tests

Prior to mechanical testing, specimens were smoothed out to remove any surface imperfections. Then, to define the geometric density of each sample, mass and sizes were measured.

The effects of the degrading actions were evaluated in terms of the variation in the mechanical properties of the reference values which had been determined for non-degraded specimens. The flexural strength values ($\sigma_{f,max}$) of prismatic samples were measured on a three-point bending configuration (bottom span of 60 mm) on five replicates (Palmero et al. 2015). In accordance with EN 196-1 (European Committee for Standardization 2016a) and ASTM C348 (ASTM International 2014), compressive strength ($\sigma_{c,max}$) was measured on the two residual parts resulting from the flexural test, thus on ten replicates. Flexural and compressive strength tests were performed by employing an electro-pneumatic testing machine equipped with a 50-kN loading cell applying a constant strain rate of 0.25 and 0.5 mm/min respectively.

Considering the six fines (UND1, RC, RA, BT, NA, and UND2), four degradation conditions (none, immersion in water, CaCl₂, and F/T), two different thermal treatments during curing (20 °C and 80 °C), and five replicates, a total of 240 specimens were prepared. As a result, a total of 240 flexural and 480 compressive strength tests were carried out.

RESULTS AND DISCUSSION

Density

Table 3 reports the average density of AA specimens at 28 days of curing (according to Fig. 4 cured for at least 21-days at RH > 90%) and immediately before performing the mechanical tests. Samples exposed to the 48-hour treatment at 80 °C always exhibit lower density values than those cured at room temperature.

It is worth noting that the average density of AA-UND1 cured at room temperature (1986 kg/m³) is exactly equal to the value obtained by averaging the densities of the single constituents RC, RA, BT, and NA (1987 kg/m³). Accordingly, the average density values of the AA-UND1 and AA-UND2 specimens (cured at 20 °C) are very similar. In contrast, if one considers the average densities of heat-cured specimens, the value of AA-UND1 (1929 kg/m³) is not equivalent or close to the average density values of the four main components (1877 kg/m³). It suggests that individual components tend to behave differently to the AA-UND1 sample because of the heat treatment. This assertion can

also be confirmed by the disparity in density between AA-UND1 and AA-UND2 (exposed to the 80 °C treatment).

Specimens made up of AA-NA show the highest densities consistent with the values of ρ_p in Table 2. Despite the AA-BT particles being characterized by high particle density values, the low density of AA samples evidences their poor packing ability due to the irregular morphology of these particles (Letelier et al. 2018). This aspect is confirmed by the high intergranular porosity shown by the AA-BT dry compact in Table 2.

Flexural and compressive strength results

Fig. 5 depicts the ratio between flexural and compressive strength ($\sigma_{f,max}/\sigma_{c,max}$). In the case of products cured entirely at 20 °C (Fig. 5-a), the average value of $\sigma_{f,max}/\sigma_{c,max}$ varies from 0.21 of AA-RC to 0.45 of AA-RA and AA-NA. Similarly, thermally-cured specimens at 80 °C (Fig. 5-b) exhibited average flexural and compressive strength ratios ranging from 0.21 to 0.43. Considering all the results, one may postulate that $\sigma_{f,max}$ accounts for 30% on average of $\sigma_{c,max}$ with a standard deviation of $\pm 10\%$, in line with literature (Kheder and Al-Windawi 2005; Haach et al. 2011). For this reason, the discussion concerning the effects of degradation has been limited to the compressive strength results, with the assumption that any conclusions drawn could also apply to flexural strength values.

Effect of immersion in water

Specimens cured at 20 °C

The effect of immersion in water on the compressive strength of AA-CDW fines cured at 20 °C is illustrated in Fig. 6-a.

AA samples from both undivided fractions UND1 and UND2 did not show any evidence of degradation following immersion in distilled water and no deterioration in mechanical properties were recorded. In contrast, AA-UND1 showed a significant increase in strength after being exposed to water, thus revealing the tendency for the continuous development of hardening reactions in the mixture. The coexistence of different mechanisms such as the alkali-activation of the

aluminosilicates, the hydration of unreacted cementitious particles and pozzolanic reactions between residual $\text{Ca}(\text{OH})_2$ and silica species can be accounted for by the mechanical strength of AA-UND1 and AA-UND2 fractions and their heightened resistance to degradation by immersion in water (Kovler 2001; Bassani et al. 2019a; Bassani et al. 2019b; Lau Hiu Hoong et al. 2021). The presence of RC fraction in both AA-UND1 and AA-UND2 mixtures substantially contributed to the gain in strength, since non-degraded AA-RC specimens (cured at 20 °C) reached compressive strength values which were almost double that of the other fractions. Moreover, AA-RC specimens were affected, albeit only slightly, by immersion in water degradation with the statistically significant reduction in $\sigma_{c,\max}$ (t-test results: $t_{17} = 4.06$, $p < 0.001$) limited to an average of 8% with respect to non-degraded specimens. Immersion in water favoured the re-hydration of residual cementitious particles present in AA-RC and compensated for any possible deterioration due to the immersion in water (Bassani et al. 2016).

The RA constituent displayed the lowest average compressive strength values. However, AA-RA specimens cured at 20 °C did not show a reduction in mechanical properties as a result of water degradation. Specifically, AA-RA specimens after 5 days of immersion in water revealed a significant increase in their compressive strength from 3.0 MPa for the reference samples to 4.6 MPa recorded for the water immersed specimens (t-test results: $t_{16} = -29.8$, $p < 0.001$). The performance of the AA-RA material cured at 20 °C can be partially ascribed to its greater compactness with respect to other fines (Table 2), which makes it less susceptible to water penetration. Furthermore, the waterproofing properties (Zhu et al. 2014) of residual bitumen compounds in RA could have prevented or partially prevented water penetrating into the open voids of hardened material, thus minimizing any damage caused.

Specimens made up of AA-BT and AA-NA powders treated at 20 °C were negatively affected by water since both fractions suffered a significant reduction in their mechanical properties after immersion in water for 5 days ($\sigma_{c,\max}$ of BT and NA specimens decreased by 55 and 24%, respectively, with respect to the values of non-degraded samples). This behaviour can be attributed to the low magnitude of the alkali-activation reaction which led to an unstable and weakly-bonded structure. This assumption is compatible with the significant loss of particles experienced by AA-BT

specimens at the end of the degradation stage, which can be regarded as an exhibition of stripping phenomena caused by water in the porous and weak solid structure.

Specimens cured at 80 °C

Mechanical results in Fig. 6-b evidence that the 48-hour heat treatment at 80 °C during curing promoted alkali-activation reactions since all hardened specimens showed markedly enhanced mechanical properties in comparison to specimens cured at 20 °C without treatment (Tefa et al. 2021). Nevertheless, heat-treated AA products were more markedly degraded than the corresponding mixtures cured at room temperature.

In contrast to the results for specimens treated at 20 °C (Fig. 6-a), the strength values of AA-UND1 and AA-UND2 declined due to water degradation. Thermally treated AA-UND1 exhibited an average decrease of 43% in compressive strength properties after water immersion, while the thermally treated AA-UND2 showed a strength loss of about 54%.

The hydraulic stability of AA materials is still a subject of debate in literature (Coppola et al. 2020b). Some studies have pointed out that the excess of alkaline species, especially in precursors with a low content of Ca, could be the origin for their solubility in water, leading to ineffective binding and, consequently, erosion of their mechanical properties, and/or even the complete disintegration of specimens (Celerier et al. 2018; Bădănoiu et al. 2015; Ahmari and Zhang 2013). Moreover, the high solubility of unreacted AS led to diminished mechanical properties after immersion in water. In contrast, the presence of unreacted cement particles and the occurrence of pozzolanic reactions resulted in materials which were more water-resistant (Bernal and Provis 2014; Celerier et al. 2018; Coppola et al. 2020a; Ahmari and Zhang 2013; Hanjitsuwan et al. 2018).

In addition to these considerations, the deterioration in the mechanical properties of products subjected to treatment at 80 °C can be partially associated with the low density of specimens (Table 3). In this configuration, the higher volume of voids facilitated the penetration of water and resulting degradation.

The behaviour of UND1 specimens cured at 80 °C is also reflected in the behaviour of its constituents. Apart from AA-RC, the AA-RA, AA-BT, and AA-NA materials experienced a significant decrease in compressive strength values following immersion in water. The average $\sigma_{c,max}$ of AA-RA

specimens exposed to water degradation was reduced by 70% in comparison to non-degraded reference materials. Similarly, NA material experienced a high degree of water degradation judging by the fall in compressive strength from 15.8 MPa for non-degraded specimens to 2.2 MPa for the deteriorated ones.

The drastic deterioration in the mechanical properties of both the RA and NA specimens can be attributed to the swelling phenomena experienced by hardened products during their immersion in water. The expansion in volume caused superficial cracking and particle detachments. This was probably caused by the formation of expansive products in the presence of water, i.e. hydrated silica (Coppola et al. 2020a). Some studies pointed out that the high alkalinity of the AS leads to reactive products which are comparable to those deriving from the alkali-silica reactions of OPC (Williamson and Juenger 2016; Li et al. 2019). The formation of these hydrated products probably contributed to the expansive behaviour recorded in RA and NA specimens when immersed in water.

Consistent with other materials, the BT fraction which was exposed to the 48-hour 80 °C thermal treatment also saw its compressive strength halved after immersion in water, albeit no visible signs of cracking or swelling phenomena were detected. Komnitsas et al. (2015) attributed the decrease in strength of alkali-activated ceramic materials after immersion in water to the depolymerisation of the aluminosilicate matrix.

RC fines (thermally treated during curing) exhibited the lowest strength reduction (-13%) due to immersion in water. The higher resistance of the RC component compensated for the poor behaviour of the other components (RA, BT, and NA) in the undivided mixtures (UND1 and UND2). Indeed, the loss in strength sustained by the water-degraded UND1 and UND2 specimens was slightly lower than that sustained by the RA, BT, and NA materials.

The better performance of the AA-RC mixtures cured at 80 °C can again be attributed to the formation of hardened products which do not dissolve in water. The low content of aluminosilicates and the significant amount of CaO in RC (Table 1) suggests that the development of the mechanical properties of this constituent are due in large part to the re-hydration of residual cement particles. It is worth observing that the average $\sigma_{c,max}$ value displayed by specimens cured at 80 °C (for 48 hours)

was significantly higher at the 95% of confidence level than that of specimens cured at 20 °C (i.e. $\sigma_{c,max} = 20.1$ MPa at 20 °C; $\sigma_{c,max} = 21.8$ MPa at 80 °C; t-test results: $t_{18} = -3.21$, $p = 0.005$).

Effect of de-icing salts

Specimens cured at 20 °C

Fig. 7 shows the variation in compressive strength between reference specimens and those immersed in an aqueous solution of calcium chloride for the simulation of de-icing salt degradation.

As regards the AA materials cured at 20 °C, the effect of immersion in the CaCl₂ solution leads to results comparable to those observed in the case of immersion in water. Both undivided fractions (UND1 and UND2) cured at 20 °C were not influenced by the degradation of the CaCl₂ solution. Consistent with the results of Fig. 6-a, these materials exhibited a slight improvement in their mechanical property values after immersion in the CaCl₂ solution. The behaviour of UND1 specimens is mainly influenced by the effects of immersion in the CaCl₂ solution as observed on their constituent materials (AA-RC, -RA, -BT, and -NA). Specimens produced with AA-RC fines and cured at 20 °C displayed no variation in compressive strength in comparison to non-degraded reference fines. Meanwhile, the immersion of the AA-BT and AA-NA samples cured at 20 °C in a CaCl₂ aqueous medium caused a decrease in their mechanical properties of around 30% when compared to reference mixtures. AA-RA specimens treated at 20 °C showed excellent resistance to CaCl₂ solution degradation, increasing their strength by 55% with respect to non-degraded references.

Specimens cured at 80 °C

As observed with immersion in water degradation, AA materials subjected to the 80 °C heat-treatment experienced a drastic reduction in their mechanical properties after exposure to the CaCl₂ solution (Fig. 7-b). Most of the AA products showed a reduction in excess of 50% after CaCl₂ degradation. Only AA-RC and AA-UND1 managed to restrict their losses in compressive strength to 27 and 48% respectively in comparison to reference mixtures. Analogously to water degradation, the immersion of AA-RA and AA-NA specimens in the CaCl₂ solution caused noticeable swelling and

detachment phenomena which led to a severe deterioration of these materials and to the almost total loss of mechanical strength.

De-icing salts are known to produce some deleterious effects in cementitious materials (Colleparidi et al. 1994). Although the actual process by which the material is damaged is not well defined, some studies indicated that CaCl_2 can react with Ca(OH)_2 to form calcium oxychloride which can impair the hydrated cement structure (Suraneni et al. 2017; Suraneni et al. 2018; Qiao et al. 2018). Chatterji (1978) reported that the leaching of Ca(OH)_2 from cementitious binders makes them more porous and more susceptible to water penetration and expansion phenomena caused by water freezing. To the best of the authors' knowledge, the effects of de-icing salt degradation on AA binders have not been discussed in literature.

On examination of the compressive strength results (Fig. 7), it is evident that the detrimental effects of de-icing salt exposure are approximately equivalent to those caused by immersion in water (Fig. 6) independently of the curing temperature. It is believed that calcium is predominantly present as calcite in RA, NA and BT raw powders, and therefore not responsible for this detrimental reaction (Bassani et al. 2019a). Although a fraction of residual calcium oxide and hydroxide may be present in RC, it is reasonable to assume that these compounds reacted with silicates during the AA process, and are thus not available for this degradation mechanism (Coppola et al. 2020c).

The greater decrease in compressive strength values of specimens exposed to the 80 °C thermal treatment can be explained by their immersion in water: (i) the solubility of unreacted AS in the pores of materials, (ii) the depolymerisation of the aluminosilicate matrix, and (iii) the higher porosity of specimens due to the heat treatment at 80 °C.

Effect of freeze/thaw cycles

Specimens cured at 20 °C

From an examination of the results in Fig. 8, it would appear that not all the AA fines are influenced by the F/T degradation. Independently of curing temperature and materials, after 12 F/T cycles all specimens exhibited higher strength values than the reference ones. In the case of specimens prepared at 20 °C (Fig. 8-a), both AA-UND1 and AA-UND2 exhibited an adequate resistance to F/T

degradation. Their performance can be viewed as intermediate when considering the performance range for all four main constituents.

The higher mechanical strength values recorded after F/T degradation can be ascribed to the longer curing time of degraded specimens with respect to the reference ones. Considering that the F/T degradation process lasted for 12 cycles of 2 days each, degraded specimens underwent mechanical characterization after 52 days (28 days of curing + 24 days of F/T degradation) in comparison to 28 days for the reference samples. This additional time allowed for the development of geopolymerization and, possibly, hydration reactions in a not-deleterious curing environment, providing a boost to mechanical strength.

Specimens cured at 80 °C

The F/T cycles did not produce a detrimental effect on the 80 °C heat-cured AA materials (Fig. 8-b). However, in this case, the post degradation increase in strength was less prominent than that for specimens cured at 20 °C. The average $\sigma_{c,max}$ value for AA-UND1 increased by 7% after F/T cycles, while for AA-UND2 the increase observed was 14%.

It is recognized that the F/T degradation was not as severe as per the usual F/T experimental protocols, e.g., ASTM C666 (ASTM International 2015) and CEN/TS 12390-9 (European Committee for Standardization 2016b), owing to the fact that the specimens were not saturated (Brooks et al. 2010). In this investigation, F/T cycles were applied to partially saturated material as a more realistic simulation of field conditions for road applications (Bassani and Tefa 2018; Bozyurt et al. 2013; Khoury and Zaman 2007).

Durability assessment

To synthetically evaluate the effect of each type of degradation on the mechanical properties of AA products, a durability index (DI) was defined as per the following eq. 1:

$$DI(x) = \frac{\sigma_{c,max}(x)}{\sigma_{c,max}(ref.)} \quad \text{eq.1}$$

where x indicates the type of degradation, $\sigma_{c,max}(ref.)$ is the compressive strength of the reference mixture (i.e. not exposed to degradation), $\sigma_{c,max}(x)$ is the average compressive strength of specimens after the x degradation.

DI values reported in Table 4 are supported by the results coming from the independent sample t-test. This approach facilitated an assessment of the differences between the mean compressive strength values of degraded samples and non-degraded ones with the level of significance of these differences evidenced by symbols associated with the p-value range. The results indicate that DI values around the unit fail to depict any significant differences between the two sample groups compared. Conversely, when DI assumes values far from the unit value, the differences between groups become significant. Hence, DI is an index which is robust enough to interpret the results coming from degrading actions. When DI is higher than or at least equal to 1, the material strength is not affected by the degradation process, so it exhibits good durability. Conversely, when DI is lower than 1 the material is suffering from the detrimental actions of the applied degradation process.

The DI values of 80 °C heat-cured samples were always lower than or equal to those relating to materials cured at 20 °C. Although the 48-hour thermal exposure treatment at 80 °C during curing considerably increased their mechanical properties, these AA products were strongly affected by water and CaCl₂ degradations. Except for AA-RC, the degradation caused by immersion in water and CaCl₂ significantly compromised the mechanical properties of heat-treated specimens, whose DI values ranged between 0.57 and 0.14. In the case of 80 °C treated materials, the AA-RA and AA-NA fractions resulted as the most vulnerable constituents, exhibiting the lowest DI values.

Both UND1 and UND2 specimens displayed the highest DI values, at least in the case of specimens entirely cured at 20 °C. Considering that heat treatments are not always a viable option in road constructions, the more robust response to degradation simulation in the case of curing at 20 °C (compared to materials exposed to the thermal treatment at 80 °C) is a very positive aspect

of this specific application. The AA-UND1 sample, which includes practically all the fine particles present in mixed CDW aggregates achieved intermediate strength values because of the AA and curing at room temperature. Meanwhile, since AA-UND1 proved so resistant to the effects of degradation actions and retained its strength, this material can be regarded as a durable phase which acts to stabilize recycled CDW aggregates for use in subbase road pavements.

According to DI outputs, independently of the curing conditions, all materials responded well to the effects of F/T degradation, due to the low severity of the action applied. However, the adopted degradation procedure is more simulative of the real degrading actions that can occur in road applications. In pavement structures, materials employed in subbase layers are not directly exposed to the F/T action in saturated conditions, since they are below impervious layers and far from the groundwater. For this reason, the saturation state (which can be reached by completely immersing specimens in water) is not representative of real conditions.

CONCLUSIONS

The experimental study investigated the level of degradation due to immersion in water, chemical attacks by CaCl_2 , and freeze/thaw (F/T) action on specimens produced from the AA of the finest fraction ($d < 0.125$ mm) of CDW aggregates. Since the finest fraction is more reactive and susceptible to undergoing alkali-activation, the degradation assessment was carried out on samples made up of AA fines to exclude any secondary effects due to other mixture-related factors.

The effects of degrading actions were evaluated in terms of variation in mechanical strength values between degraded specimens and reference (non-degraded) ones. CDW aggregate constituents (i.e., RC, RA, BT, and NA) were compared with samples obtained from the two undivided fractions (UND1 and UND2). Based on the obtained results, the following conclusions can be drawn:

- AA fines cured at 80 °C for 48 hours were characterized by lower densities than those cured at room temperature, due to water evaporation during the heating treatment;

- alkali-activation reactions were favoured during heat curing of the aluminosilicate-rich constituents (i.e. BT, UND1 and UND2) since the strength of specimens containing such precursors was significantly greater than that of the same materials cured at 20 °C;
- AA-RC specimens did not suffer any degradation due to immersion in water independently of curing temperature since the re-hydration of residual cement particles favoured the hydraulic stability of these products. In contrast, AA specimens containing other constituents (RA, BT, NA, UND1, and UND2) and exposed to 80 °C for 48 hours proved more vulnerable to degradation than the corresponding mixtures cured at 20 °C. It is reasonable to suppose that immersion in water caused the solubilization of the products resulting from the AA process;
- AA-RA and AA-NA treated at 80 °C exhibited extensive swelling phenomena after immersion in water, causing superficial cracking and spalling. Therefore, the mechanical strengths of these specimens experienced a drastic reduction after the degradation caused by immersion in water;
- the decrease in mechanical properties of AA specimens after immersion in CaCl₂ solution was approximately equivalent to that recorded for water-degraded specimens independently of curing temperature. It suggests that the effect of CaCl₂ on mechanical strength values was not greater than the degradation caused by immersion in water.

The robust performance throughout the degradation simulation displayed by AA-UND1 and AA-UND2 fractions cured at 20 °C can be considered a great result for the specific application of road constructions in situations where heat treatments are not viable. UND1 samples attained intermediate strength values following AA and curing without any thermal treatment, and managed to retain these values in spite of the application of degrading actions. Therefore, the fine fraction of unseparated CDW aggregates can successfully stabilize coarse aggregate mixtures ($d \geq 0.125$ mm) and retain their properties even after exposure to water immersion, CaCl₂ solution, and the F/T process.

DATA AVAILABILITY STATEMENT

All data, models, and code generated or used during the study appear in the submitted article.

ACKNOWLEDGEMENTS

The authors would like to thank Ms. Federica Arcidiacono and Mr. Davide Guglielmo for their support with part of this research activity. The recycled aggregates were provided by Cavit S.p.A., while the alkaline solution was provided by INGESSIL S.r.l., all of whom are gratefully acknowledged for their support.

REFERENCES

- Agrela, F., Barbudo, A., Ramírez, A., Ayuso, J., Carvajal, M. D., and Jiménez, J. R. (2012). "Construction of road sections using mixed recycled aggregates treated with cement in Malaga, Spain." *Resources, Conservation and Recycling*, 58, 98–106.
- Ahmari, S., and Zhang, L. (2013). "Durability and leaching behavior of mine tailings-based geopolymer bricks." *Construction and Building Materials*, 44, 743–750.
- Allahverdi, A., and Kani, E. N. (2013). "Use of construction and demolition waste (CDW) for alkali-activated or geopolymer cements." *Handbook of recycled concrete and demolition waste*, Woodhead Publishing Series in Civil and Structural Engineering, Elsevier, 439–475.
- Angulo, S. C., Ulsen, C., John, V. M., Kahn, H., and Cincotto, M. A. (2009). "Chemical–mineralogical characterization of C&D waste recycled aggregates from São Paulo, Brazil." *Waste Management*, 29(2), 721–730.
- Arulrajah, A., Mohammadinia, A., D'Amico, A., and Horpibulsuk, S. (2017). "Cement kiln dust and fly ash blends as an alternative binder for the stabilization of demolition aggregates." *Construction and Building Materials*, 145, 218–225.
- Arulrajah, A., Mohammadinia, A., Phummiphan, I., Horpibulsuk, S., and Samingthong, W. (2016). "Stabilization of Recycled Demolition Aggregates by Geopolymers comprising Calcium Carbide Residue, Fly Ash and Slag precursors." *Construction and Building Materials*, 114, 864–873.
- Assi, L. N., Eddie Deaver, E., and Ziehl, P. (2018). "Effect of source and particle size distribution on the mechanical and microstructural properties of fly Ash-Based geopolymer concrete." *Construction and Building Materials*, 167, 372–380.
- ASTM International. (2012). *Standard Test Method for Scaling Resistance of Concrete Surfaces Exposed to Deicing Chemicals*. ASTM C672-12.
- ASTM International. (2014). *Standard Test Method for Flexural Strength of Hydraulic-Cement Mortars*. ASTM C348-14.
- ASTM International. (2015). *Standard Test Method for Resistance of Concrete to Rapid Freezing and Thawing*. ASTM C666-15.
- Avirneni, D., Peddinti, P. R. T., and Saride, S. (2016). "Durability and long term performance of geopolymer stabilized reclaimed asphalt pavement base courses." *Construction and Building Materials*, 121, 198–209.
- Bădănoiu, A. I., Abood Al-Saadi, T. H., and Voicu, G. (2015). "Synthesis and properties of new materials produced by alkaline activation of glass cullet and red mud." *International Journal of Mineral Processing*, 135, 1–10.
- Bassani, M., Riviera, P. P., and Tefa, L. (2016). "Short-Term and Long-Term Effects of Cement Kiln Dust Stabilization of Construction and Demolition Waste." *Journal of Materials in Civil Engineering*, 29(5), 04016286.

- Bassani, M., and Tefa, L. (2018). "Compaction and freeze-thaw degradation assessment of recycled aggregates from unseparated construction and demolition waste." *Construction and Building Materials*, 160, 180–195.
- Bassani, M., Tefa, L., Coppola, B., and Palmero, P. (2019a). "Alkali-activation of aggregate fines from construction and demolition waste: Valorisation in view of road pavement subbase applications." *Journal of Cleaner Production*, 234, 71–84.
- Bassani, M., Tefa, L., Russo, A., and Palmero, P. (2019b). "Alkali-activation of recycled construction and demolition waste aggregate with no added binder." *Construction and Building Materials*, 205, 398–413.
- Bernal, S. A., and Provis, J. L. (2014). "Durability of Alkali-Activated Materials: Progress and Perspectives." *Journal of the American Ceramic Society*, (D. J. Green, ed.), 97(4), 997–1008.
- Bianchini, G., Marrocchino, E., Tassinari, R., and Vaccaro, C. (2005). "Recycling of construction and demolition waste materials: a chemical–mineralogical appraisal." *Waste Management*, 25(2), 149–159.
- Bilodeau, J.-P., Doré, G., and Schwarz, C. (2011). "Effect of seasonal frost conditions on the permanent strain behaviour of compacted unbound granular materials used as base course." *International Journal of Pavement Engineering*, 12(5), 507–518.
- Bilsen, V., Kretz, D., Padilla, P., Van Acoleyen, M., Van Ostaeyen, J., Olga Izdebska, Eggert Hansen, M., Bergmans, J., and Szuppinger, P. (2018). *Development and implementation of initiatives fostering investment and innovation in construction and demolition waste recycling infrastructure*. Final Report, IDEA Consult, Brussels, Belgium, 206.
- Bozyurt, O., Keene, A. K., Tinjum, J. M., Edil, T. B., and Fratta, D. (2013). "Freeze-Thaw Effects on Stiffness of Unbound Recycled Road Base." *Mechanical Properties of Frozen Soil*, H. Zubeck and Z. Yang, eds., ASTM International, 100 Barr Harbor Drive, PO Box C700, West Conshohocken, PA 19428-2959, 1–19.
- Brooks, R., Bahadory, M., Tovia, F., and Rostami, H. (2010). "Properties of alkali-activated fly ash: high performance to lightweight." *International Journal of Sustainable Engineering*, Taylor & Francis, 3(3), 211–218.
- Camargo, F. F., Edil, T. B., and Benson, C. H. (2013). "Strength and stiffness of recycled materials stabilised with fly ash: a laboratory study." *Road Materials and Pavement Design*, 14(3), 504–517.
- Cardoso, R., Silva, R. V., Brito, J. de, and Dhir, R. (2016). "Use of recycled aggregates from construction and demolition waste in geotechnical applications: A literature review." *Waste Management*, 49, 131–145.
- Celerier, H., Jouin, J., Tessier-Doyen, N., and Rossignol, S. (2018). "Influence of various metakaolin raw materials on the water and fire resistance of geopolymers prepared in phosphoric acid." *Journal of Non-Crystalline Solids*, 500, 493–501.
- Chatterji, S. (1978). "Mechanism of the CaCl₂ attack on portland cement concrete." *Cement and Concrete Research*, 8(4), 461–467.
- Collepari, M., Coppola, L., and Pistolesi, C. (1994). "Durability of Concrete Structures Exposed to CaCl₂ Based Deicing Salts." *Special Publication*, 145, 107–120.
- Coppola, B., Palmero, P., Montanaro, L., and Tulliani, J.-M. (2020a). "Alkali-activation of marble sludge: Influence of curing conditions and waste glass addition." *Journal of the European Ceramic Society*, 40(11), 3776–3787.
- Coppola, B., Tulliani, J.-M., Antonaci, P., and Palmero, P. (2020b). "Role of Natural Stone Wastes and Minerals in the Alkali Activation Process: A Review." *Materials*, 13(10), 2284.
- Coppola, L., Coffetti, D., Crotti, E., Gazzaniga, G., and Pastore, T. (2020c). "The Durability of One-Part Alkali-Activated Slag-Based Mortars in Different Environments." *Sustainability*, 12(9), 3561.
- Courard, L., Rondeux, M., Zhao, Z., and Michel, F. (2020). "Use of Recycled Fine Aggregates from C&DW for Unbound Road Sub-Base." *Materials*, 13(13), 2994.
- Cristelo, N., Fernández-Jiménez, A., Vieira, C., Miranda, T., and Palomo, Á. (2018). "Stabilisation of construction and demolition waste with a high fines content using alkali activated fly ash." *Construction and Building Materials*, 170, 26–39.
- Cunningham, M. A., Snyder, E., Yonkin, D., Ross, M., and Elsen, T. (2008). "Accumulation of deicing salts in soils in an urban environment." *Urban Ecosystems*, 11(1), 17–31.

- Degirmenci, F. N. (2017). "Freeze-thaw and fire resistance of geopolymer mortar based on natural and waste pozzolans." *Ceramics - Silikaty*, 41–49.
- van Deventer, J. S. J., Provis, J. L., Duxson, P., and Brice, D. G. (2010). "Chemical Research and Climate Change as Drivers in the Commercial Adoption of Alkali Activated Materials." *Waste and Biomass Valorization*, 1(1), 145–155.
- Di Maria, A., Eyckmans, J., and Van Acker, K. (2018). "Downcycling versus recycling of construction and demolition waste: Combining LCA and LCC to support sustainable policy making." *Waste Management*, 75, 3–21.
- Duxson, P., Fernández-Jiménez, A., Provis, J. L., Lukey, G. C., Palomo, A., and van Deventer, J. S. J. (2007). "Geopolymer technology: the current state of the art." *Journal of Materials Science*, 42(9), 2917–2933.
- European Committee for Standardization. (2008a). *Tests for mechanical and physical properties of aggregates - Part 7: Determination of the particle density of filler - Pyknometer method. EN 1097-7:2008.*
- European Committee for Standardization. (2008b). *Tests for mechanical and physical properties of aggregates - Part 4: Determination of the voids of dry compacted filler. EN 1097-4:2008.*
- European Committee for Standardization. (2016a). *Methods of testing cement - Part 1: Determination of strength. EN 196-1:2016.*
- European Committee for Standardization. (2016b). *Testing hardened concrete - Part 9: Freeze-thaw resistance with de-icing salts - Scaling. CEN/TS 12390-9:2016.*
- European Environment Agency. (2020). *Construction and demolition waste: challenges and opportunities in a circular economy.* Briefing Report, European Environment Agency, Copenhagen, Denmark.
- Farnam, Y., Dick, S., Wiese, A., Davis, J., Bentz, D., and Weiss, J. (2015). "The influence of calcium chloride deicing salt on phase changes and damage development in cementitious materials." *Cement and Concrete Composites*, 64, 1–15.
- Guo, H., Shi, C., Guan, X., Zhu, J., Ding, Y., Ling, T.-C., Zhang, H., and Wang, Y. (2018). "Durability of recycled aggregate concrete – A review." *Cement and Concrete Composites*, 89, 251–259.
- Haach, V. G., Vasconcelos, G., and Lourenço, P. B. (2011). "Influence of aggregates grading and water/cement ratio in workability and hardened properties of mortars." *Construction and Building Materials*, 25(6), 2980-2987.
- Hanjitsuwan, S., Phoo-ngernkham, T., Li, L., Damrongwiriyanupap, N., and Chindaprasirt, P. (2018). "Strength development and durability of alkali-activated fly ash mortar with calcium carbide residue as additive." *Construction and Building Materials*, 162, 714–723.
- Huda, S. B., and Shahria Alam, M. (2015). "Mechanical and Freeze-Thaw Durability Properties of Recycled Aggregate Concrete Made with Recycled Coarse Aggregate." *Journal of Materials in Civil Engineering*, 27(10), 04015003.
- Juenger, M. C. G., Winnefeld, F., Provis, J. L., and Ideker, J. H. (2011). "Advances in alternative cementitious binders." *Cement and Concrete Research*, 41(12), 1232–1243.
- Karlsson, R., & Isacson, U. (2006). Material-related aspects of asphalt recycling — state-of-the-art. *Journal of Materials in Civil Engineering*, 18(1), 81-92.
- Katz, A. (2003). "Properties of concrete made with recycled aggregate from partially hydrated old concrete." *Cement and Concrete Research*, 33(5), 703–711.
- Kheder, G. F., and Al-Windawi, S. A. (2005). "Variation in mechanical properties of natural and recycled aggregate concrete as related to the strength of their binding mortar." *Materials and Structures*, 38(281), 701–709.
- Khoury, N. N., and Zaman, M. M. (2007). "Environmental Effects on Durability of Aggregates Stabilized with Cementitious Materials." *Journal of Materials in Civil Engineering*, 19(1), 41–48.
- Komnitsas, K. (2016). "Co-valorization of marine sediments and construction and demolition wastes through alkali activation." *Journal of Environmental Chemical Engineering*.
- Komnitsas, K., and Zaharaki, D. (2007). "Geopolymerisation: A review and prospects for the minerals industry." *Minerals Engineering*, 20(14), 1261–1277.

- Komnitsas, K., Zaharaki, D., Vlachou, A., Bartzas, G., and Galetakis, M. (2015). "Effect of synthesis parameters on the quality of construction and demolition wastes (CDW) geopolymers." *Advanced Powder Technology*, 26(2), 368–376.
- Kovler, K. (2001). "Enhancing Water Resistance of Cement and Gypsum-Cement Materials." *Journal of Materials in Civil Engineering*, 13(5), 349–355.
- Lau Hiu Hoong, J. D., Hou, Y., Turcry, P., Mahieux, P.-Y., Hamdoun, H., Amiri, O., Lux, J., and Aït-Mokhtar, A. (2021). "Reactivity of Recycled Aggregates Used for Pavement Base: From Field to Laboratory." *Journal of Materials in Civil Engineering*, American Society of Civil Engineers, 33(6), 04021129
- Lee, K. Y., Kodikara, J., and Bouazza, A. (2004). "Modeling and Laboratory Assessment of Capillary Rise in Stabilized Pavement Materials." *Transportation Research Record: Journal of the Transportation Research Board*, 1868(1), 3–13.
- Letelier, V., Ortega, J., Muñoz, P., Tarela, E., and Moriconi, G. (2018). "Influence of Waste Brick Powder in the Mechanical Properties of Recycled Aggregate Concrete." *Sustainability*, 10(4), 1037.
- Li, C., Sun, H., and Li, L. (2010). "A review: The comparison between alkali-activated slag (Si+Ca) and metakaolin (Si+Al) cements." *Cement and Concrete Research*, 40(9), 1341–1349.
- Li, Z., Thomas, R. J., and Peethamparan, S. (2019). "Alkali-silica reactivity of alkali-activated concrete subjected to ASTM C 1293 and 1567 alkali-silica reactivity tests." *Cement and Concrete Research*, 123, 105796.
- Limbachiya, M. C., Marrocchino, E., and Koulouris, A. (2007). "Chemical–mineralogical characterisation of coarse recycled concrete aggregate." *Waste Management*, 27(2), 201–208.
- Loria, H., Pereira-Almao, P., and Satyro, M. (2009). "Prediction of Density and Viscosity of Bitumen Using the Peng–Robinson Equation of State." *Industrial & Engineering Chemistry Research*, 48(22), 10129–10135.
- McLellan, B. C., Williams, R. P., Lay, J., van Riessen, A., and Corder, G. D. (2011). "Costs and carbon emissions for geopolymer pastes in comparison to ordinary portland cement." *Journal of Cleaner Production*, 19(9–10), 1080–1090.
- Mirza, S. (2006). "Durability and sustainability of infrastructure — a state-of-the-art report." *Canadian Journal of Civil Engineering*. 33(6): 639-649.
- Mohammadinia, A., Arulrajah, A., Sanjayan, J., Disfani, M. M., Bo, M. W., and Darmawan, S. (2014). "Laboratory Evaluation of the Use of Cement-Treated Construction and Demolition Materials in Pavement Base and Subbase Applications." *Journal of Materials in Civil Engineering*, 27(6), 04014186.
- Mohammadinia, A., Arulrajah, A., Sanjayan, J., Disfani, M. M., Win Bo, M., and Darmawan, S. (2016). "Stabilization of Demolition Materials for Pavement Base/Subbase Applications Using Fly Ash and Slag Geopolymers: Laboratory Investigation." *Journal of Materials in Civil Engineering*, 28(7), 04016033.
- Pacheco-Torgal, F., Abdollahnejad, Z., Camões, A. F., Jamshidi, M., and Ding, Y. (2012). "Durability of alkali-activated binders: A clear advantage over Portland cement or an unproven issue?" *Construction and Building Materials*, 30, 400–405.
- Palmero, P., Formia, A., Antonaci, P., Brini, S., and Tulliani, J.-M. (2015). "Geopolymer technology for application-oriented dense and lightened materials. Elaboration and characterization." *Ceramics International*, 41(10), 12967–12979.
- Palmero, P., Formia, A., Tulliani, J.-M., and Antonaci, P. (2017). "Valorisation of alumino-silicate stone muds: From wastes to source materials for innovative alkali-activated materials." *Cement and Concrete Composites*, 83, 251–262.
- Panizza, M., Natali, M., Garbin, E., Tamburini, S., and Secco, M. (2018). "Assessment of geopolymers with Construction and Demolition Waste (CDW) aggregates as a building material." *Construction and Building Materials*, 181, 119–133.
- Puthussery, J. V., Kumar, R., and Garg, A. (2017). "Evaluation of recycled concrete aggregates for their suitability in construction activities: An experimental study." *Waste Management*, 60, 270–276.

- Qiao, C., Suraneni, P., and Weiss, J. (2018). "Flexural strength reduction of cement pastes exposed to CaCl₂ solutions." *Cement and Concrete Composites*, 86, 297–305.
- Reig, L., Tashima, M. M., Borrachero, M. V., Monzó, J., Cheeseman, C. R., and Payá, J. (2013). "Properties and microstructure of alkali-activated red clay brick waste." *Construction and Building Materials*, 43, 98–106.
- Robayo-Salazar, R. A., Rivera, J. F., and Mejía de Gutiérrez, R. (2017). "Alkali-activated building materials made with recycled construction and demolition wastes." *Construction and Building Materials*, 149, 130–138.
- Ruiz-Santaquiteria, C., Fernández-Jiménez, A., Skibsted, J., and Palomo, A. (2013). "Clay reactivity: Production of alkali activated cements." *Applied Clay Science*, 73, 11–16.
- Saiz Martínez, P., González Cortina, M., Fernández Martínez, F., and Rodríguez Sánchez, A. (2016). "Comparative study of three types of fine recycled aggregates from construction and demolition waste (CDW), and their use in masonry mortar fabrication." *Journal of Cleaner Production*, 118, 162–169.
- Sangsefidi, E., Wilson, D. J., Larkin, T. J., and Black, P. M. (2019). "The Role of Water in Unbound Granular Pavement Layers: a Review." *Transportation Infrastructure Geotechnology*, 6(4), 289–317.
- Silva, H. M. R. D., Oliveira, J. R. M., and Jesus, C. M. G. (2012). "Are totally recycled hot mix asphalts a sustainable alternative for road paving?" *Resources, Conservation and Recycling*, 60, 38–48.
- Sun, Z., Cui, H., An, H., Tao, D., Xu, Y., Zhai, J., and Li, Q. (2013). "Synthesis and thermal behavior of geopolymer-type material from waste ceramic." *Construction and Building Materials*, 49, 281–287.
- Suraneni, P., Azad, V. J., Isgor, O. B., and Weiss, J. (2018). "Role of Supplementary Cementitious Material Type in the Mitigation of Calcium Oxychloride Formation in Cementitious Pastes." *Journal of Materials in Civil Engineering*, 30(10), 04018248.
- Suraneni, P., Monical, J., Unal, E., Farnam, Y., and Weiss, J. (2017). "Calcium Oxychloride Formation Potential in Cementitious Pastes Exposed to Blends of Deicing Salt." *ACI Materials Journal*, 114(4).
- Tefa, L., Bassani, M., Coppola, B., and Palmero, P. (2021). "Strength development and environmental assessment of alkali-activated CDW fines. Towards the exploitation of the unselected fraction in stabilized recycled road materials." *Construction and Building Materials*, 289, 123017.
- Temuujin, J., Williams, R. P., and van Riessen, A. (2009). "Effect of mechanical activation of fly ash on the properties of geopolymer cured at ambient temperature." *Journal of Materials Processing Technology*, 209(12–13), 5276–5280.
- Tian, S., Tang, L., Ling, X., Kong, X., Li, S., and Cai, D. (2019). "Cyclic behaviour of coarse-grained materials exposed to freeze-thaw cycles: Experimental evidence and evolution model." *Cold Regions Science and Technology*, 167, 102815.
- Topçu, İ. B., Toprak, M. U., and Uygunoğlu, T. (2014). "Durability and microstructure characteristics of alkali activated coal bottom ash geopolymer cement." *Journal of Cleaner Production*, 81, 211–217.
- Vásquez, A., Cárdenas, V., Robayo, R. A., and de Gutiérrez, R. M. (2016). "Geopolymer based on concrete demolition waste." *Advanced Powder Technology*, 27(4), 1173–1179.
- Williamson, T., and Juenger, M. C. G. (2016). "The role of activating solution concentration on alkali-silica reaction in alkali-activated fly ash concrete." *Cement and Concrete Research*, 83, 124–130.
- Zaharaki, D., Galetakis, M., and Komnitsas, K. (2016). "Valorization of construction and demolition (C&D) and industrial wastes through alkali activation." *Construction and Building Materials*, 121, 686–693.
- Zhu, J., Birgisson, B., and Kringos, N. (2014). "Polymer modification of bitumen: Advances and challenges." *European Polymer Journal*, 54, 18–38.

FIGURES

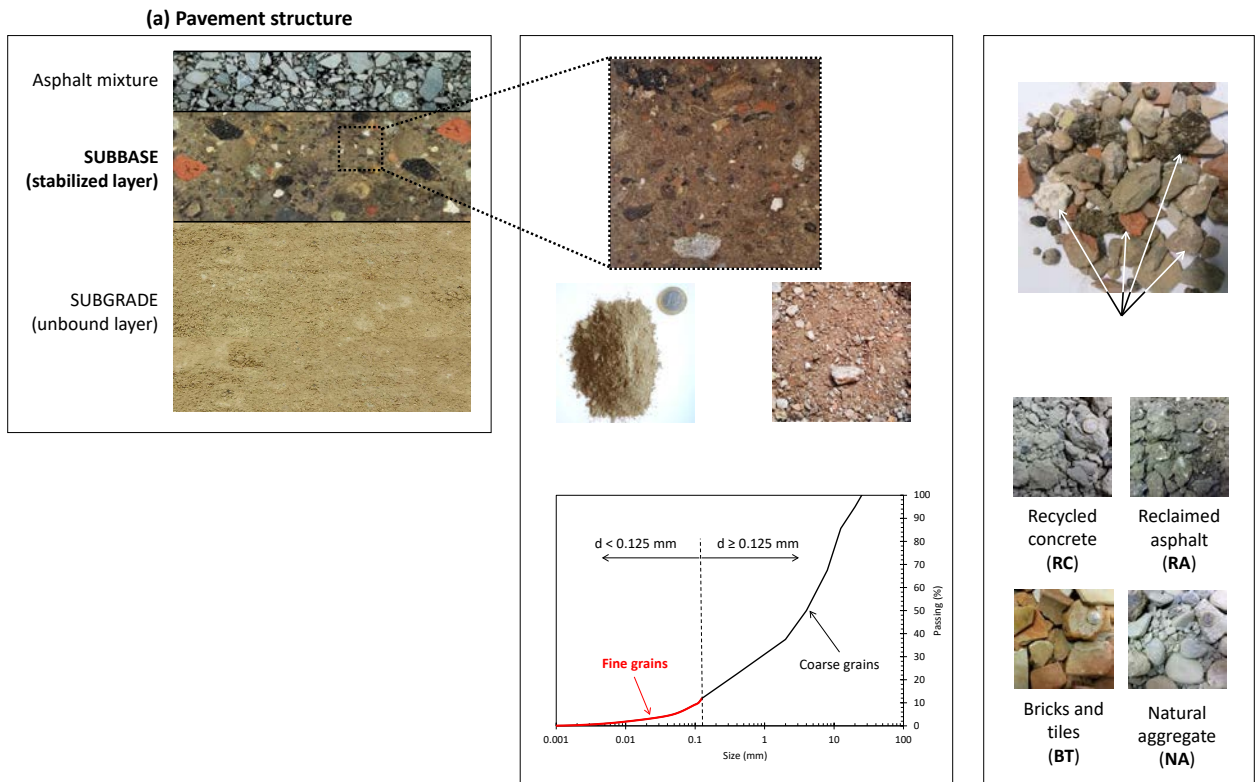


Fig. 1. General overview of the use of CDW aggregates in the formation of stabilized subbase road pavement layers: (a) pavement structure, (b) stabilized subbase layer with CDW aggregates, (c) constituents of CDW coarse aggregates

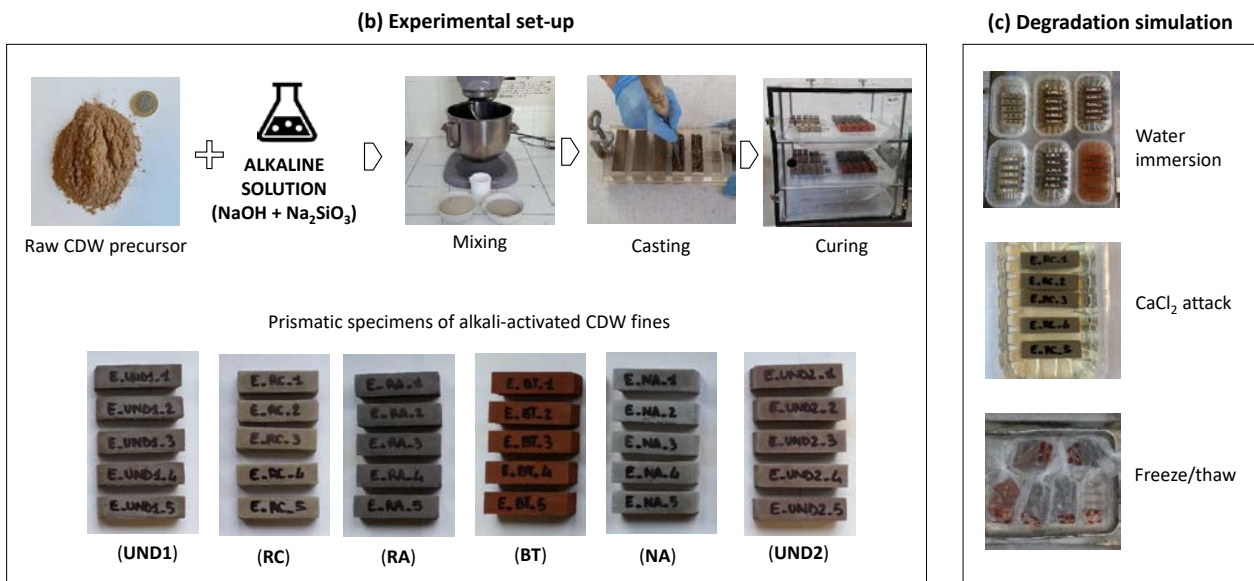
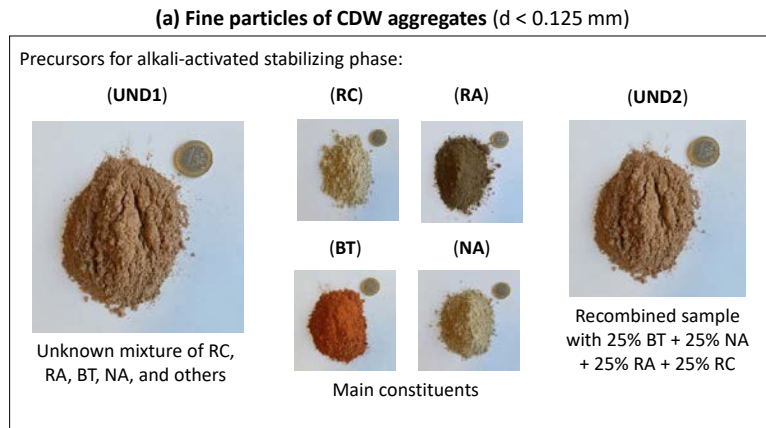


Fig. 2. Research concept. (a) Details of CDW fine particles employed as precursor for AA to form the stabilizing phase; (b) experimental set-up; (c) durability assessment of alkali-activated CDW fines

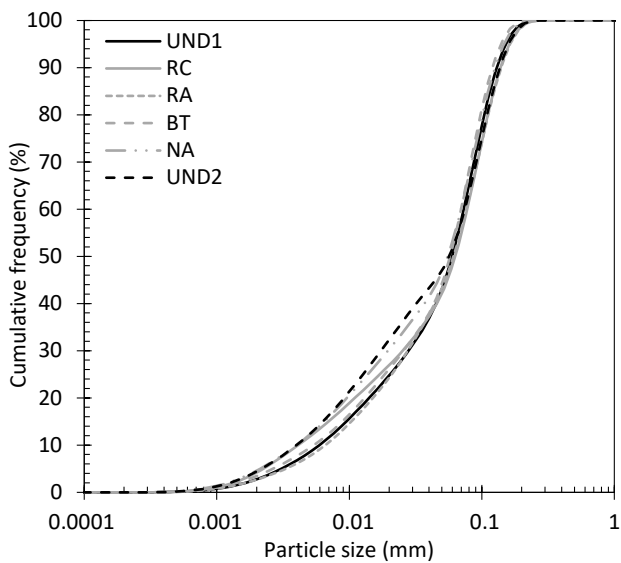
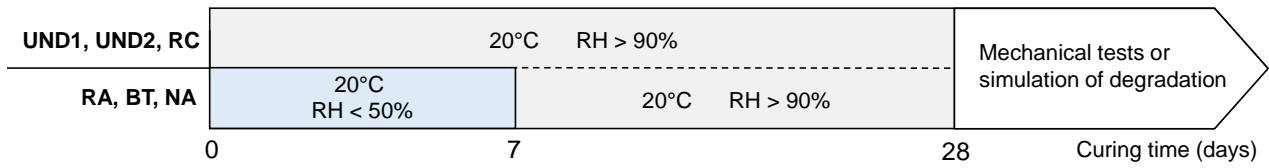
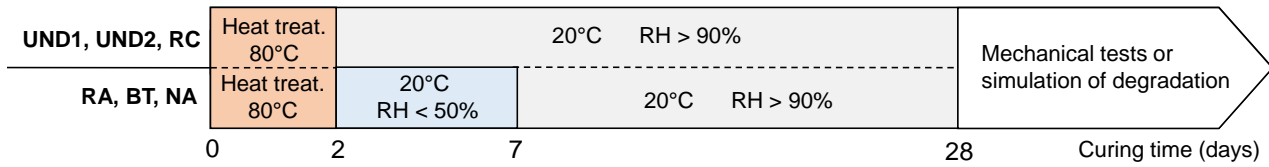


Fig. 3. Particle size distribution of size-recombined CDW powders (combination of 50% in mass of $d < 0.063$ mm and $0.063 \leq d < 0.125$ mm)

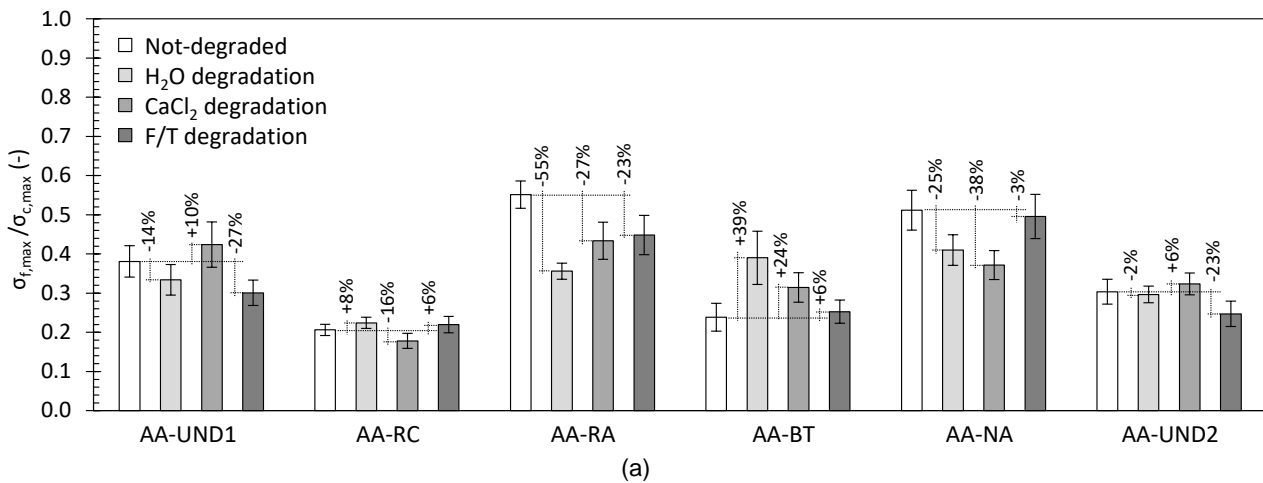


(a)

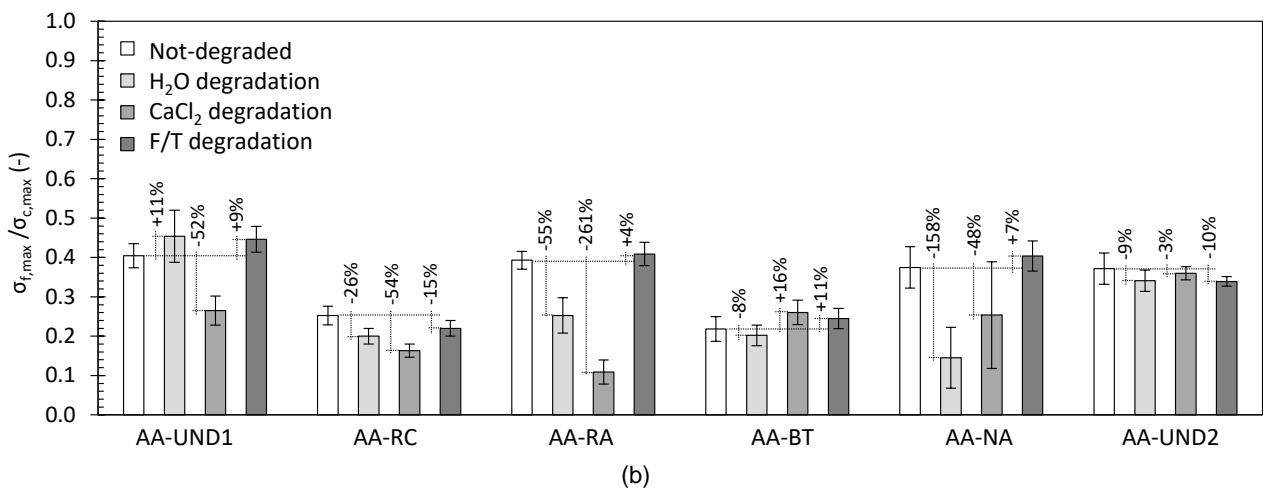


(b)

Fig. 4. Outline of curing conditions (a) without and (b) with heat treatment at 80 °C depending on the constituent



(a)



(b)

Fig. 5. Ratio between average flexural and compressive strength values of specimens cured at (a) 20 °C and (b) 80 °C (error bars indicate one standard deviation of each ratio and are obtained as per the error propagation theory). The percentage indicates the variation in the non-degraded value for each category of material

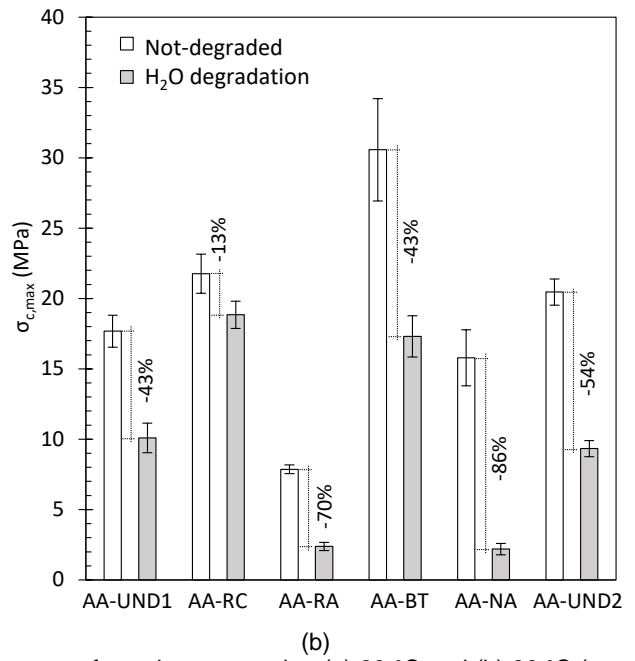
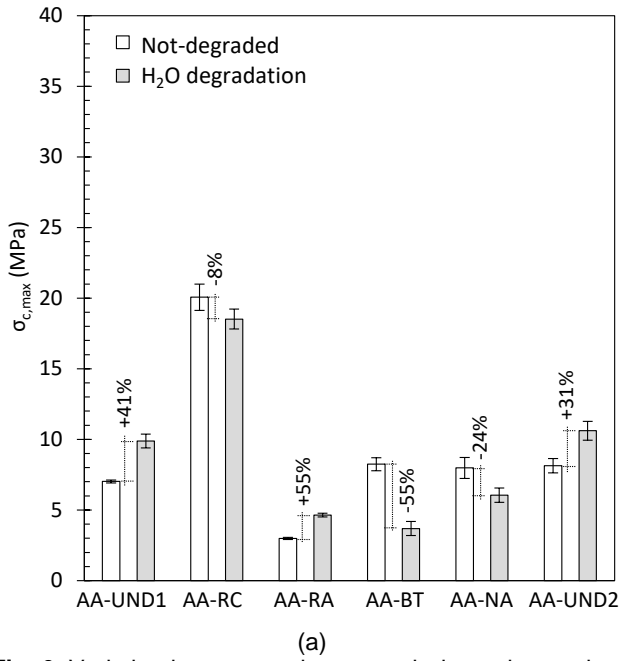


Fig. 6. Variation in compressive strength due to immersion in water of specimens cured at (a) 20 °C and (b) 80 °C (error bars indicate one standard deviation)

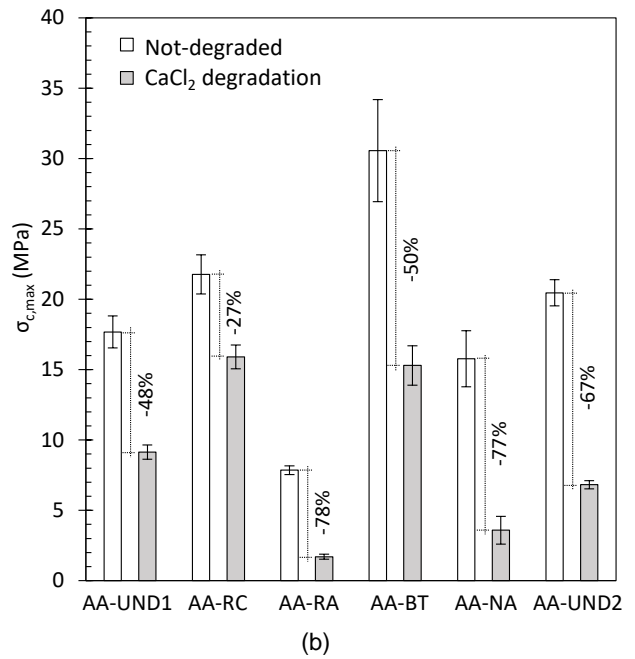
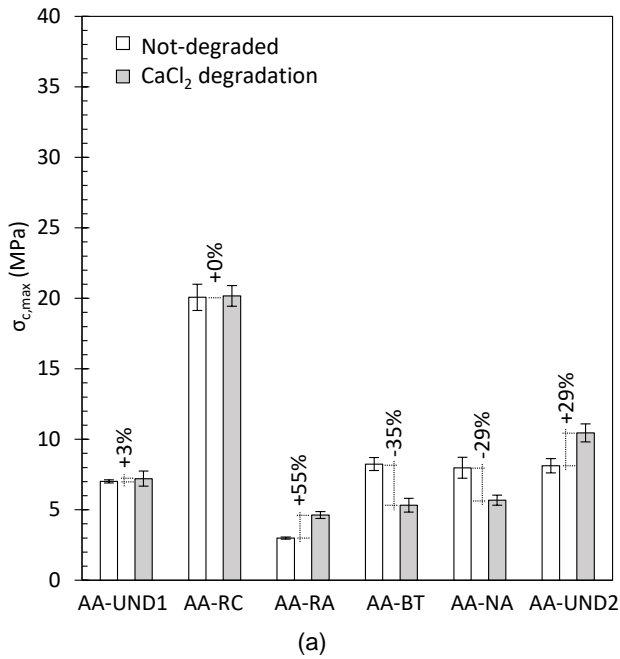


Fig. 7. Variation in compressive strength due to CaCl₂ degradation on specimens cured at (a) 20 °C and (b) 80 °C (error bars indicate one standard deviation)

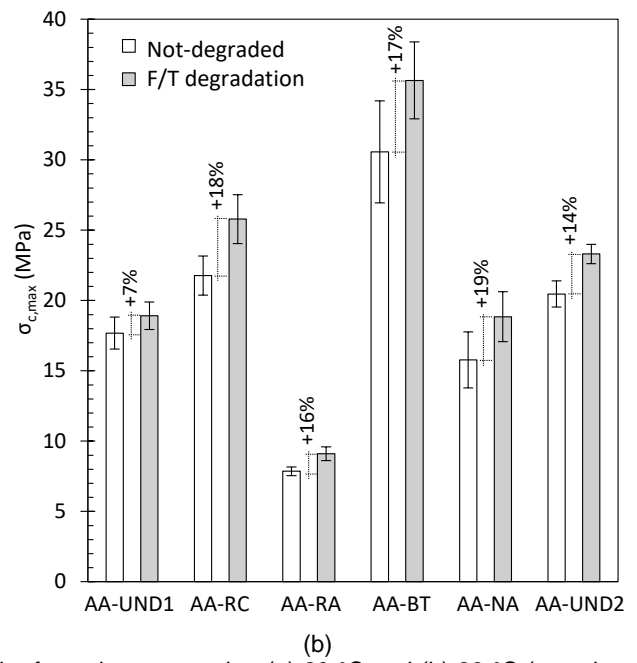
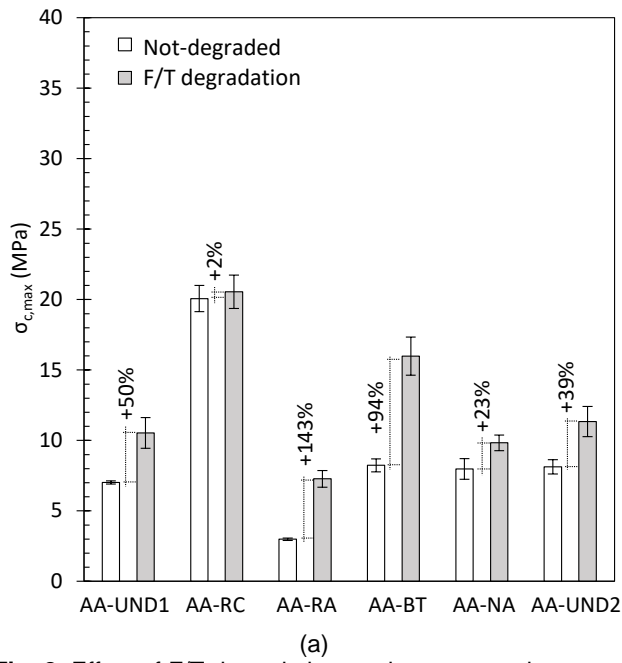


Fig. 8. Effect of F/T degradation on the compressive strength of specimens cured at (a) 20 °C and (b) 80 °C (error bars indicate one standard deviation)

LIST OF FIGURES

Fig. 1. General overview of the use of CDW aggregates in the formation of stabilized subbase road pavement layers: (a) pavement structure, (b) stabilized subbase layer with CDW aggregates, (c) constituents of CDW coarse aggregates

Fig. 2. Research concept. (a) Details of CDW fine particles employed as precursor for AA to form the stabilizing phase; (b) experimental set-up; (c) durability assessment of alkali-activated CDW fines

Fig. 3. Particle size distribution of size-recombined CDW powders (combination of 50% in mass of $d < 0.063$ mm and $0.063 \leq d < 0.125$ mm)

Fig. 4. Outline of curing conditions (a) without and (b) with heat treatment at 80 °C depending on the constituent

Fig. 5. Ratio between average flexural and compressive strength values of specimens cured at (a) 20 °C and (b) 80 °C (error bars indicate one standard deviation of each ratio and are obtained as per the error propagation theory). The percentage indicates the variation in the non-degraded value for each category of material

Fig. 6. Variation in compressive strength due to immersion in water of specimens cured at (a) 20 °C and (b) 80 °C (error bars indicate one standard deviation)

Fig. 7. Variation in compressive strength due to CaCl_2 degradation on specimens cured at (a) 20 °C and (b) 80 °C (error bars indicate one standard deviation)

Fig. 8. Effect of F/T degradation on the compressive strength of specimens cured at (a) 20 °C and (b) 80 °C (error bars indicate one standard deviation)

TABLES

Table 1. XRF results for CDW fines

Element	Mass (%)					
	UND1	RC	RA	BT	NA	UND2
SiO ₂	38.3	36.3	32.8	59.1	37.8	40.7
Al ₂ O ₃	12.23	5.90	6.78	18.3	6.08	8.70
CaO	9.78	23.5	5.65	4.66	14.5	11.8
CO ₂	24.4	20.9	37.0	0.00	22.9	21.4
Fe ₂ O ₃	4.11	3.16	2.91	7.07	3.86	4.20
MgO	6.0	7.51	11.00	5.06	12.2	10.7
SO ₃	1.47	1.04	0.977	0.242	0.00	0.56
K ₂ O	1.75	0.896	0.842	2.490	0.772	1.16
TiO ₂	0.544	0.323	0.263	0.957	0.290	0.407

Table 2. Particle density of CDW powders and intergranular porosity of CDW dry compacts

Constituent	Particle density ρ_p (kg/m ³)	Intergranular porosity, ν (%)
UND1	2626	33.3
RC	2574	34.5
RA	2380	26.0
BT	2752	34.3
NA	2705	30.0
UND2	2566	31.2

Table 3. Average geometric density values of AA specimens at the end of curing stage (before degradation simulation or mechanical tests)

Curing temp. (°C)	Density, mean \pm standard deviation (kg/m ³)					
	AA-UND1	AA-RC	AA-RA	AA-BT	AA-NA	AA-UND2
20	1986 \pm 14	2037 \pm 22	1971 \pm 16	1797 \pm 28	2144 \pm 16	1993 \pm 19
80	1929 \pm 15	1959 \pm 14	1849 \pm 7	1688 \pm 11	2010 \pm 26	1874 \pm 19

Table 4. Durability index (DI) for AA products depending on the type of precursor. Independent sample t-test statistics are reported to assess the hypothesis that the reference mean strength values of non-degraded samples and samples subjected to degradation are significantly different at the 95% confidence level: (**) $p < 0.001$, (*) $0.001 \leq p \leq 0.05$, (°) $p > 0.05$

Curing temp. (°C)	Degradation	Specimens					
		AA-UND1	AA-RC	AA-RA	AA-BT	AA-NA	AA-UND2
20	Water	1.41**	0.92**	1.55**	0.45**	0.76**	1.31**
	CaCl ₂	1.03°	1.00°	1.55**	0.65**	0.71**	1.29**
	F/T	1.50**	1.02°	2.43**	1.94**	1.23**	1.39**
80	Water	0.57**	0.87**	0.30**	0.57**	0.14**	0.46**
	CaCl ₂	0.52**	0.73**	0.22**	0.50**	0.23**	0.33**
	F/T	1.07*	1.18**	1.16**	1.17*	1.19*	1.14**